

Confocal chromatic sensor with actively tilted lens for 3D measurement

MARTIN E. FUERST,^{1,*} CHRISTIAN HAIDER,¹ ERNST CSENCICS,¹
AND GEORG SCHITTER¹

¹Christian Doppler Laboratory for Precision Engineering for Automated In-Line Metrology, Automation and Control Institute (ACIN), Technische Universität Wien, 1040 Vienna, Austria

*martin.fuerst@tuwien.ac.at

Abstract: Confocal chromatic displacement sensors are versatile and precise sensors for measuring the distance to a single point. In order to obtain a 3D measurement device, this paper presents an integrated scanning sensor design, which employs a tilting lens mechanism for manipulating the light path of the sensor. The optical implications of the design are analytically modeled and simulated. An experimental setup is constructed to evaluate the system design and to test its performance on a variety of samples. Results show good agreement with the simulations and modeling, with maximal tip/tilt angles of $\pm 2.5^\circ$, the setup is capable of measuring a volume of $1.5 \times 1.5 \times 1 \text{ mm}^3$ with a lateral resolution of $8.7 \text{ }\mu\text{m}$ and an axial resolution of 28 nm .

© 2020 Optical Society of America

1. Introduction

Three-dimensional measurement technology is becoming increasingly important for quality assurance in production processes [1–3]. Optical measurement principles offer several advantages for this purpose as they are contact-less and provide high precision as well as short measurement times [4,5]. The non-contacting properties are of special interest in dimensional measurements of delicate parts, such as optical components, and they facilitate the operation in challenging environments such as vacuum, high temperatures or industrial surroundings [6]. Laser triangulation sensors are a popular example for an optical distance sensor as they achieve high throughput and a resolution down to 30 nm [7]. Confocal chromatic sensors offer even higher axial resolution, down to 10 nm , and measurement spot sizes of a few micrometers [8]. Another advantage of the confocal chromatic principle is its capability to simultaneously measure distance to, as well as the thickness of, a sample [9].

One way to obtain the desired 3D measurement systems is to combine an optical distance sensor with an external positioning device such as linear stages, coordinate measurement machines or belt systems [10–12]. This positioning device can either move the sample or the sensor to obtain volumetric data of a sample area. In both cases the achievable throughput is typically limited by the achievable bandwidth of the positioning system, which crucially depends on the mass that needs to be moved [13].

Another approach, that has been presented recently, manipulates solely the *optical path* of the sensor by integrating fast steering mirrors or galvanometer scanners [14–16]. This eliminates the need of moving the entire sensor head, enabling faster, more reliable and more compact integrated measurement systems. However, this approach requires the space between the sensor head and the sample to be sufficiently large in order to accommodate the scanning device. In the case of a confocal chromatic sensor, this dictates the use of a sensor with a rather large working distance and thus a low numerical aperture. This also compromises the achievable resolution and angular acceptance of the sensor, as these parameters depend on a high numerical aperture of the optical system. For high-precision metrology systems, additional hardware between the lens and the sample should thus be avoided.

The contribution of this paper is the concept, design, analysis and experimental validation of a

compact, integrated scanning confocal chromatic 3D sensor comprising a tilting lens mechanism, which replaces a mirror-based scanner for manipulating the light path. The tilting motion is equivalent to moving the light source relative to the optical axis of the lens and is thus shifting the measurement spot. Potential benefits of such a system are highly integrated package sizes, allowing for scanning operation without sacrificing resolution as well as a potentially higher scan speed compared to conventional designs due to the reduced moving mass. Equations to estimate the scan range and measurement volume of the proposed 3D sensor design are derived, ray-tracing simulations are performed to investigate aberrations in the system, and an experimental setup is developed to demonstrate the feasibility of the proposed design.

2. Scanning-lens confocal chromatic sensor

2.1. Confocal chromatic sensor principle

The confocal chromatic sensor (CCS) employs the confocal principle and longitudinal chromatic aberration to measure distances [17]. Figure 1a sketches the principal setup. A broadband light source is focused on a pinhole which is imaged on the sample surface. Due to the chromatic aberration, each wavelength is focused in a different image plane. The reflected light is directed towards a spectrometer via a beamsplitter. In this receiving light path, there is a second pinhole, which ensures that only light that was in focus on the sample surface passes to the spectrometer. The recorded spectrum exhibits a peak at the wavelength corresponding to the sample distance.

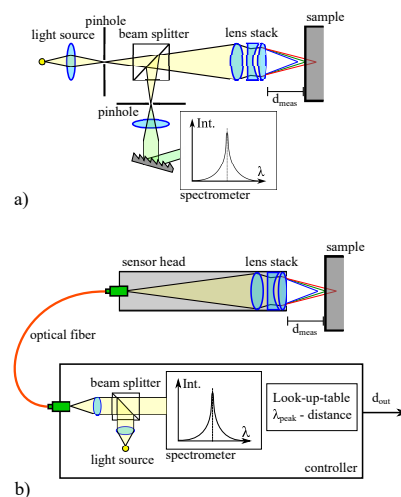


Fig. 1: Working principle of a confocal chromatic sensor. a) Basic setup with the confocal principle selecting the wavelength that passes to the spectrometer. b) Industrial realization where the sensor head is separated from the controller unit and an optical fiber replaces the pinholes.

For samples that consist of multiple layers with different refractive indices, the confocal chromatic sensor is also capable of one-sided thickness measurements. This means that the thickness of a sample can be measured without the need to position a second distance sensor on the other side of the sample. Each surface reflects the wavelength that is in focus and the spectrometer then records multiple peaks at different wavelengths. For thickness measurements, the refractive indices of the materials need to be known.

To increase the versatility and portability of the sensor design, the components are typically

distributed between a controller unit and a sensor head, as shown in Fig. 1b. The controller unit contains the lightsource, the beamsplitter and the spectrometer, while the sensor head contains the lens stack. These two parts are connected by an optical fiber, which effectively replaces the two pinholes.

2.2. Tilting lens design

In order to manipulate the optical path without adding elements after the optical lens stack of a confocal chromatic sensor (CCS), a concept with an actively tilted lens is developed. Tilting the lens is equivalent to moving the point light source relative to the optical axis, which in turn changes the position of the focused measurement spot. The conventional sensor design in Fig. 1b shows the standard layout of a CCS sensor head, comprising a fiber coupler, a lens stack and a housing for alignment. Fig. 2a shows this optical layout, reduced to its principal components: A light source and a (tiltable) optical stack. For modeling the assembly, the layout is further simplified in Fig. 2b by using a thick lens approximation for the optical stack and defining the point of rotation at the intersection of the optical axis with the first principal plane.

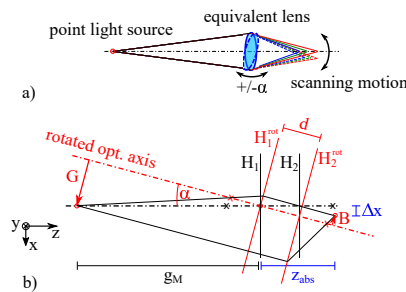


Fig. 2: Concept of the tilted-lens confocal chromatic sensor (CCS). a) Reduced optical layout of a confocal chromatic sensor head. b) Labelled thick-lens approximation of the imaging light path.

Utilizing paraxial approximations [18], the following relations for the location of the measurement spot can be derived when tilting the lens around an axis in the first principal plane:

$$\Delta x = d \cdot \sin(\alpha) \quad (1)$$

$$z_{abs} = \frac{f \cdot g_M}{\cos(\alpha) \cdot g_M - f} + d \cdot \cos(\alpha) \quad (2)$$

with d the distance between the principal planes H_1 and H_2 , f being the focal length (measured from the second principal plane) and g_M the initial distance of the light source to the first principal plane. Δx is the displacement of the measurement spot with respect to the initial optical axis. z_{abs} denotes the axial position of the measurement spot with respect to the first principal plane. Relating the axial position to its initial position $z_{init} = d + \frac{f \cdot g_M}{g_M - f}$ gives the relative shift Δz of the measurement spot:

$$\Delta z = z_{abs} - z_{init} = \frac{f \cdot g_M}{\cos(\alpha) \cdot g_M - f} - \frac{f \cdot g_M}{g_M - f} + d \cdot (\cos(\alpha) - 1). \quad (3)$$

These relations enable to estimate the scan field and the scanner bow of a tilted-lens confocal chromatic sensor design. Equation (1) shows that the lateral scan range depends solely on the principal plane distance which depends on, and typically increases with, the number of

optical elements in the lens stack [19]. Equation (2) is made up of two terms: one that increases in magnitude for larger tilt angles α and one that decreases for larger tilt angles. For exemplary values of $d = 18$ mm, $g_M = 90$ mm, $f = 5$ mm, which are typical for state-of-the-art confocal chromatic sensors [20], and $\alpha_{max} = 2.5^\circ$, the resulting scan range is $x_{scan} = 2 \cdot \Delta x_{max} = 2 \cdot d \cdot \sin(\alpha_{max}) = 1.57$ mm. The resulting scanner bow for the same parameters results to $\Delta z_{max} = 0.0118$ mm.

3. Simulations

For verification of the modeling and analysis presented in the previous section, ray-tracing simulations are performed. The MatLab Add-On Optometrika [21] is used as basis and is adapted in order to simulate a simplified CCS. Figure 3a displays the optical layout implemented for simulation. It consists of a point light source, an aperture, a plano-convex lens and a screen. The aperture is placed 90 mm from the light source and has an open diameter of 14 mm. The spherical lens consists of D-LAK6 glass, has a curvature radius of 10.5 mm and is placed 92 mm from the light source ($g_M = 92$ mm). The lens geometry results in a focal length of $f = 13.54$ mm and a principal plane distance of $d = 1.52$ mm. The screen is used to detect the position of the measurement spot by varying its axial position and identifying the screen position at which the bundle of rays intersecting the screen has the smallest cross-section. The dimensions of the elements and the distances are chosen to resemble the simplified version of a typical confocal displacement sensor, containing only a single lens.

Simulations are performed for three wavelengths (465 nm, 549 nm and 710 nm), representing the start, middle and end of the measurement range of the confocal sensor. Each of these wavelengths is simulated with 20.000 rays to investigate the size and shape of the scan volume.

Figure 3b illustrates the resulting scan-field of the scanning CCS for tilt angles of $\pm 3^\circ$. The lateral scan range is about 220 μm , the axial scan range is about 470 μm . It can be seen that the scanner bow results in a measurement volume that is not a perfect cuboid. Effectively, this limits the usable axial scan range to 430 μm , which is given by the difference between the start of the measurement range at the 0° -position and the end of the measurement range in the outer position (compare Fig. 3b).

To compare the magnitude of the simulated scanner bow to the scanner bow from the analytical relations, equations (1) and (2) are evaluated for the simulated system parameters (d , f , g_M), as given above. Figures 3c and 3d show that the results of simulation and modeling are comparable but also show slight deviations. The calculated scanner bow (Fig. 3c) amounts to 4.3% of the scan range while the simulated scanner bow amounts to 10% of the scan range. The calculated lateral scan range (Fig. 3d) is 160 μm while the simulated scan range is 220 μm . This probably results from aberrations that are not considered in the approximations made for the analytical modeling, but do affect the ray-tracing simulations. Especially coma aberration is present in the system, since the light source is not located on the optical axis of the tilted lens.

4. Prototype setup

To investigate the feasibility of the proposed sensor design and validate the simulation and analytic results, an experimental setup is designed (see Figure 4). A commercially available high-end confocal chromatic sensor head (IFS2405-1, Micro-Epsilon Optronik, Dresden, Germany) which offers an axial resolution of 28 nm and a measurement spot size of 8 μm , is used for the experiments. The sensor head is cut in two in order to separate the fiber coupler and the lens stack. The part containing the lenses is then mounted on two orthogonally aligned rotational stages (ELL-18K/M, Thorlabs, United States), while the part containing the fiber coupler is mounted on three manual micrometer stages to facilitate alignment. The coupling fiber is connected to the Micro-Epsilon IFC2451-controller, which comprises the light source and the spectrometer. In each measurement position, the sensor remains static for 1 second, to average the distance signal

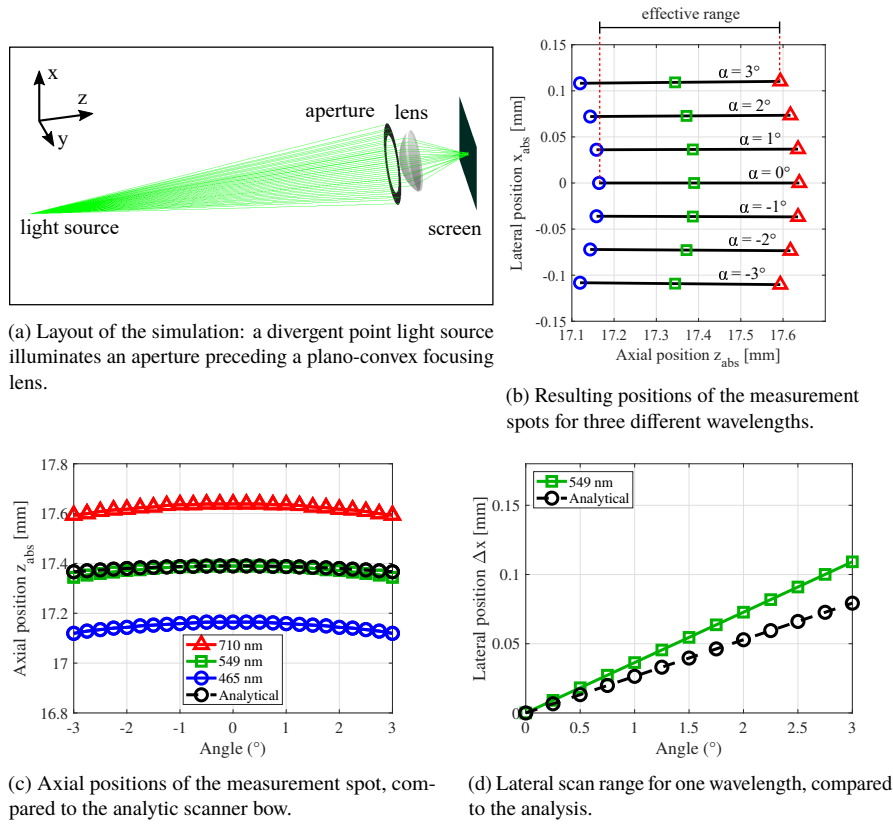


Fig. 3: Results of the ray-tracing simulations performed in MatLab.

over 1.000 values. The measured distance is transferred to a PC where data acquisition is done with MatLab. The rotational stages are also controlled via MatLab. The samples are mounted on three manual micrometer stages (XRN25P/M, Thorlabs, United States) for alignment, calibration and testing.

The rotational stages provide a bidirectional repeatability of 0.05° , which is also chosen as the step size of the scan pattern. Within the approximation of $\sin(\alpha) \approx \alpha$, this results in an evenly spaced x/y measurement-grid. The measurement range of the IFS2405-1 sensor starts at 10 mm distance from the sensor housing and ends at 11 mm from the housing. For $x_{step} = dist \cdot \sin(\alpha_{step})$, this results in a lateral step size of $8.7 \mu\text{m}$ at the start of the measurement range and $9.6 \mu\text{m}$ at the end of the measurement range. Since the spot size of the IFS2405-1 sensor is also given as $8 \mu\text{m}$, the lateral resolution of the integrated system is limited to this value. Samples are scanned point-by-point on a rectangular grid of 101×101 points evenly distributed over an angular range of -2.5° to 2.5° , corresponding to the step size of 0.05° .

A flat gauge block calibration normal (polished steel, Hoffmann Group, Munich, Germany) is scanned to investigate the scanner bow needed to calibrate the sensor system. Figure 5 shows the measurement results. In Fig. 5a, a map of the measured distance is plotted over the position angles of the rotational stages. A circular artefact can be seen that might be caused by reflections

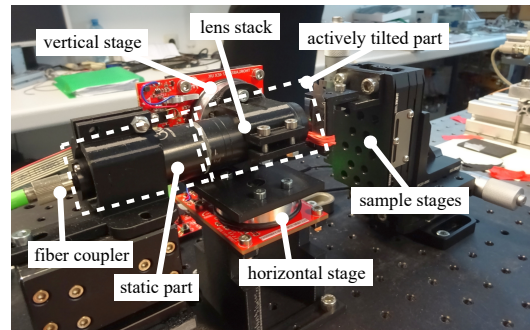
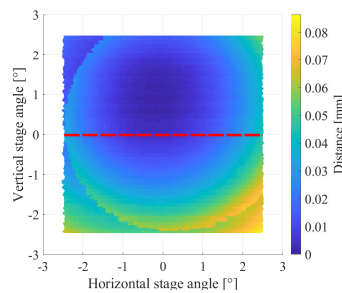
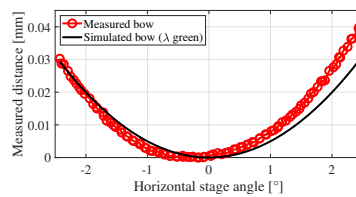


Fig. 4: Photo of the experimental setup consisting of two rotational stages and a confocal chromatic sensor head that is cut in two.

within the lens stack that arise at tilt angles higher than 2.5° . In Fig. 5b, a single line profile of the calibration measurement is compared to the simulated scanner bow. The simulation result of the medium wavelength (green) was chosen for the comparison since it is in the middle of the measurement range. It can be seen that the simulation fits the measurement quite well. There is a slight horizontal offset which is probably due to imperfect alignment of fiber coupler, lenses and rotational stages. The axial scan range is calibrated by moving the reference sample along the system axis and comparing the sensor values to the external stage values. The lateral scale is calibrated by moving a sample with a clearly visible step along the measurement range and comparing the detected position with the externally measured displacement.



(a) Measurement result of the confocal chromatic sensor.



(b) Comparison of the line indicated in a) with the simulation.

Fig. 5: Result of the calibration measurement on a flat reference sample.

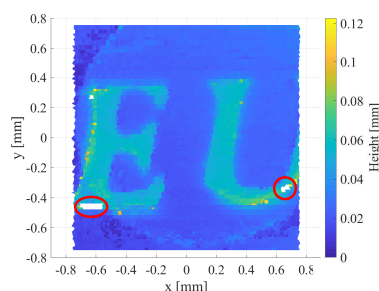
5. Experimental results

To validate the results of the analysis and the simulations, three samples with feature sizes within the scan field of the prototype system are selected and measured. The obtained results are acquired via the scanning scheme described in Section 4, are corrected for the scanner bow by subtraction of the flat gauge block sample image and are normalized by subtracting a fitted plane.

First, to demonstrate the topology measurement capabilities on a metallic surface, a part of a 20-cent Euro coin is imaged. Figure 6 shows the measurement result. The circular artefact that was present in the calibration measurement (Fig. 5a) is still visible, though reduced in magnitude. The scan field of $1.5 \times 1.5 \text{ mm}^2$ is sufficient to image parts of the embossed writing on the coin. The size of the scan field is in agreement with the values calculated in Section 2.2, as the values of the sensor used in the experiments are close to the values used for the calculations. Near the edges of the image, there are some white spots (indicated by red circles in Fig. 6b). These represent points where no distance signal could be acquired, due to insufficient intensity of the reflected light.



(a) Photograph of the sample with the scanned region indicated by the red square.

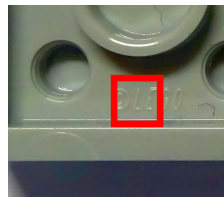


(b) Measurement result of the scanning confocal chromatic sensor. The white areas indicate measurement points where no valid values are obtained.

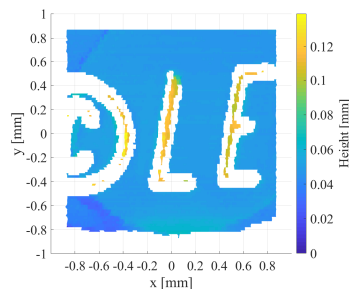
Fig. 6: Measurement result for imaging a 20-cent Euro coin.

Figure 7 shows the measurement result on the backside of a LegoTM brick, where a small company logo '©LEGO' is embossed that is barely visible with the naked eye (compare photograph in Fig. 7). With the scanning confocal chromatic sensor, the writing is clearly visible, though the edges of the embossing are too steep to provide a proper distance signal (white spots in the figure). This is due to insufficient light being reflected towards the sensor. It can also be seen that edges parallel to the y-axis are measured more reliable than edges parallel to the x-axis (see the horizontal lines of the letter 'E', for instance). This is probably caused by non-intersecting rotational axes of the stages, resulting in slightly different optical conditions for horizontal and vertical tilts.

Finally, a sample that demonstrates an industrial application of a scanning confocal chromatic



(a) Photograph of the sample with the scanned region indicated by the red square.



(b) Measurement result of the scanning confocal chromatic sensor.

Fig. 7: Measurement result of the embossed '©Lego' imprint on the backside of a Lego™-brick. The edges of the writing (white areas) are too steep to reflect enough light intensity to obtain a proper measurement signal

sensor was selected. Surface-mounted integrated circuits (SMD ICs) are connected to contact pads via bond wires. The height of the loops formed by these wires is of interest because it determines the mechanical stability of the connections [22]. Figure 8 shows the measurement result on a sample containing an IC that is connected to a board via 4 bond-wires with a wire diameter of 25 μm . As can be seen in Fig. 8, two of the loops are broken, while two are intact. The loop-height of the intact connections is about 350 μm . Automatic extraction of these parameters could allow for automatic inspection of bond-wires in an industrial setting.

In summary, it is successfully shown that by integrating a confocal chromatic sensor head with a tilting lens mechanism, a compact 3-dimensional measurement system can be obtained, with a first prototype providing a measurement volume of about $1.5 \times 1.5 \times 1 \text{ mm}^3$, a lateral resolution of 8.7 μm and an axial resolution of 28 nm.

6. Conclusion

In this paper, an integrated 3D measurement system, based on a confocal chromatic sensor with an actively tilted lens, is developed. Analytical relations to estimate the performance of the proposed system design for different setup and lens parameters are derived. The determining factor for the lateral scan range is the distance between the two principal planes of the optical stack, which typically increases with the number of optical elements in the stack. Ray-tracing simulations are in good agreement with the analysis and the feasibility of the system design is investigated by an experimental prototype setup. The experiments demonstrate that altering the optical path of a CCS by actively tilting its lens enables 3D measurement capabilities with the resulting scan volume being in good agreement with the results of analysis and simulations. For the chosen lens parameters and a scan angle of $\pm 2.5^\circ$, a measurement volume of $1.5 \times 1.5 \times 1 \text{ mm}^3$ can be obtained with a lateral resolution of 8.7 μm and an axial resolution of 28 nm. The maximum

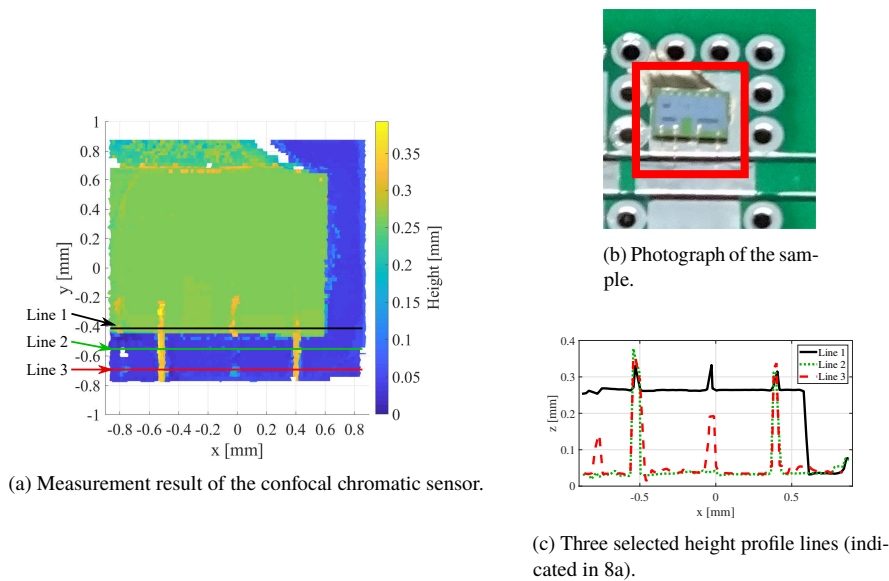


Fig. 8: Measurement result on a surface-mounted integrated circuit with two intact and two broken bond-wires. The two broken wires can be distinguished and the height of the bond-wire loops can be determined.

admissible surface slope angle can be increased by using a lens with a higher numerical aperture, which is enabled by the approach since no scanning elements between the sensor and the sample are required. Future work will be concerned with the influence of the location of the tilt axis as well as with optimization of the system geometry. Further, a strategy for high-precision calibration as well as a data-acquisition system for continuous, high-speed operation needs to be developed.

Acknowledgment

The financial support by the Christian Doppler Research Association, the Austrian Federal Ministry for Digital and Economic Affairs, and the National Foundation for Research, Technology and Development, as well as MICRO-EPSILON MESSTECHNIK GmbH & Co. KG and ATENSOR Engineering and Technology Systems GmbH is gratefully acknowledged. We also thank Johannes Schlarp, Mathias Poik and Shingo Ito (all from ACIN) for fruitful discussions.

Disclosures

The authors declare that there are no conflicts of interest related to this article.

References

1. F. Blais *et al.*, "Review of 20 years of range sensor development," *J. electronic imaging* **13**, 231–243 (2004).
2. R. Schmitt and F. Moenning, "Ensure success with inline-metrology," in *XVIII IMEKO world congress Metrology for a Sustainable Development*, (2006).
3. G. Sansoni, M. Trebeschi, and F. Docchio, "State-of-the-art and applications of 3d imaging sensors in industry, cultural heritage, medicine, and criminal investigation," *Sensors* **9**, 568–601 (2009).
4. K. Harding, *Handbook of optical dimensional metrology* (CRC Press, 2013).

5. G. Berkovic and E. Shafir, "Optical methods for distance and displacement measurements," *Adv. Opt. Photonics* **4**, 441–471 (2012).
6. X. Zou, X. Zhao, G. Li, Z. Li, and T. Sun, "Non-contact on-machine measurement using a chromatic confocal probe for an ultra-precision turning machine," *The Int. J. Adv. Manuf. Technol.* **90**, 2163–2172 (2017).
7. Micro-Epsilon Messtechnik GmbH & Co. KG, "Data sheet (<https://www.micro-epsilon.com/download/products/cat-optoncdt-en.pdf>)," optoNCDT // Laser displacement sensors (triangulation) (retrieved March 27, 2020).
8. C.-J. Weng, B.-R. Lu, P.-Y. Cheng, C.-H. Hwang, and C.-Y. Chen, "Measuring the thickness of transparent objects using a confocal displacement sensor," in *2017 IEEE International Instrumentation and Measurement Technology Conference (I2MTC)*, (IEEE, 2017), pp. 1–5.
9. A. Miks, J. Novak, and P. Novak, "Analysis of method for measuring thickness of plane-parallel plates and lenses using chromatic confocal sensor," *Appl. optics* **49**, 3259–3264 (2010).
10. M. Levoy, K. Pulli, B. Curless, S. Rusinkiewicz, D. Koller, L. Pereira, M. Ginzton, S. Anderson, J. Davis, J. Ginsberg *et al.*, "The digital michelangelo project: 3d scanning of large statues," in *Proceedings of the 27th annual conference on Computer graphics and interactive techniques*, (2000), pp. 131–144.
11. F. J. Brosed, J. J. Aguilar, D. Guillomía, and J. Santolaria, "3d geometrical inspection of complex geometry parts using a novel laser triangulation sensor and a robot," *Sensors* **11**, 90–110 (2011).
12. H. Kunzmann, T. Pfeifer, R. Schmitt, H. Schwenke, and A. Weckenmann, "Productive metrology-adding value to manufacture," *CIRP annals* **54**, 155–168 (2005).
13. R. M. Schmidt, G. Schitter, and A. Rankers, *The design of high performance mechatronics-: high-Tech functionality by multidisciplinary system integration* (Ios Press, 2014).
14. C. Yu, X. Chen, and J. Xi, "Modeling and calibration of a novel one-mirror galvanometric laser scanner," *Sensors* **17**, 164 (2017).
15. J. Schlarp, E. Csencsics, and G. Schitter, "Optical scanning of laser line sensors for 3d imaging," *Appl. optics* **57**, 5242–5248 (2018).
16. S. Ito, M. Poik, E. Csencsics, J. Schlarp, and G. Schitter, "Scanning chromatic confocal sensor for fast 3d surface characterization," in *ASPE/euspen Summer topical meeting on advancing precision in additive manufacturing. submitted for publication*, (2018).
17. G. Molesini, G. Pedrini, P. Poggi, and F. Quercioli, "Focus-wavelength encoded optical profilometer," *Opt. Commun.* **49**, 229–233 (1984).
18. M. Born and E. Wolf, *Principles of optics: electromagnetic theory of propagation, interference and diffraction of light* (Elsevier, 2013).
19. G. Schröder and H. Treiber, *Technische Optik*, vol. 8 (Vogel Buchverlag Munchen, 2007).
20. Micro-Epsilon Messtechnik GmbH & Co. KG, "Data sheet (<https://www.micro-epsilon.com/download/products/cat-confocaldt-en.pdf>)," confocalDT // Confocal chromatic sensor system (retrieved March 27, 2020).
21. Y. Petrov, "Optometrika (<https://www.github.com/caiuspetronius/optometrika>)," Github (retrieved March 27, 2020).
22. D.-B. Perng, C.-C. Chou, and S.-M. Lee, "Design and development of a new machine vision wire bonding inspection system," *The Int. J. Adv. Manuf. Technol.* **34**, 323–334 (2007).